Applied Ergonomics 62 (2017) 107–117

Contents lists available at ScienceDirect

Applied Ergonomics

journal homepage: www.elsevier.com/locate/apergo

# Ergonomic analysis of construction worker's body postures using wearable mobile sensors

Nipun D. Nath [a], Reza Akhavian [b], Amir H. Behzadan [a, *]

[a] Department of Technology and Construction Management, Missouri State University, 901 S. National Avenue, Springfield, MO 65897, USA
[b] School of Engineering, California State University, East Bay, 25800 Carlos Bee Blvd, Hayward, CA 94542, USA

ARTICLE INFO

*Article history:*
Received 4 July 2016
Received in revised form
11 February 2017
Accepted 13 February 2017
Available online 28 February 2017

*Keywords:*
Ergonomics
Construction safety
Risk assessment
Posture analysis
Smartphone sensor
Wearable technology

ABSTRACT

Construction jobs are more labor-intensive compared to other industries. As such, construction workers are often required to exceed their natural physical capability to cope with the increasing complexity and challenges in this industry. Over long periods of time, this sustained physical labor causes bodily injuries to the workers which in turn, conveys huge losses to the industry in terms of money, time, and productivity. Various safety and health organizations have established rules and regulations that limit the amount and intensity of workers' physical movements to mitigate work-related bodily injuries. A precursor to enforcing and implementing such regulations and improving the ergonomics conditions on the jobsite is to identify physical risks associated with a particular task. Manually assessing a field activity to identify the ergonomic risks is not trivial and often requires extra effort which may render it to be challenging if not impossible. In this paper, a low-cost ubiquitous approach is presented and validated which deploys built-in smartphone sensors to unobtrusively monitor workers' bodily postures and autonomously identify potential work-related ergonomic risks. Results indicates that measurements of trunk and shoulder flexions of a worker by smartphone sensory data are very close to corresponding measurements by observation. The proposed method is applicable for workers in various occupations who are exposed to WMSDs due to awkward postures. Examples include, but are not limited to industry laborers, carpenters, welders, farmers, health assistants, teachers, and office workers.



## 1. Introduction

Today's construction projects are becoming more complex and challenging. Construction workers require a wide variety of skills to be able to achieve project goals within specified time, budget, and specifications. Compared to other industries such as manufacturing, construction projects are more labor-intensive. The complexity of tasks often requires workers to go beyond their natural physical limits, or perform repetitive tasks for a long period of time. Over time, such sustained physical demand on workers' bodies may cause health issues and bodily injuries. Work-related injuries of this type are also referred to as Musculoskeletal Disorders (MSDs). Besides their adverse physical implications, MSDs can also lead to significant financial losses. For example, in 2009, direct workers' compensation costs due to MSDs were amounted to more than $50 billion in the U.S. (Liberty Mutual Research Institute For Safety, 2011). To remedy this problem, various health and safety organizations have established rules and guideline to identify the risks associated with performing certain tasks. Such efforts aim at ergonomic design of the workplace to match physical jobs with workers' natural capabilities.

### 1.1. Work-related Musculoskeletal Disorders (WMSDs)

MSDs are a group of disorders or injuries in a person's inner body parts (e.g. muscles, nerves, tendons, joints, cartilages, and spinal discs) which have relative deformations while he or she moves. Example of MSDs includes Carpal Tunnel Syndrome (CTS), Tendonitis, and Bursitis (Simoneau et al., 1996; Occupational Health Clinics for Ontario Workers Inc, 2017). Work-related Musculoskeletal Disorders (WMSDs) refer to the MSDs due to activities in the workplace associated with physical jobs.

Construction jobs are among the most ergonomically hazardous occupations which involve activities such as manual handling,

* Corresponding author.
*E-mail addresses:* nipun2016@live.missouristate.edu (N.D. Nath), reza.akhavian@csueastbay.edu (R. Akhavian), abehzadan@missouristate.edu (A.H. Behzadan).

http://dx.doi.org/10.1016/j.apergo.2017.02.007
0003-6870/

heavy lifting, body twisting, and frequently working in awkward positions, all being potential causes of WMSDs in workers (OSHA, 2000; Health and Safety Executive, 2016). According to the U.S. Department of Labor, construction is one of the six occupations where workers suffer from nonfatal occupational injuries and illnesses (Bureau of Labor Statistics, 2014). The most common types of WMSDs in construction are sprain, strain, CTS, tendonitis, and back pain. In the U.S., 32 construction workers in every 10,000 get injured from a WMSD and take leaves from work (Bureau of Labor Statistics, 2014). Among all trades of construction workers, laborers have the highest rate (45 workers in every 10,000) of getting injured due to WMSDs, with helpers, plumbers, carpenters, and others following (OSHA, 2012). In 2015, the number of days lost due to non-fatal occupational injuries in private construction sites in the U.S. was 79,890, while WMSDs incident rate per 10,000 workers was 34.6 with 13 median days away from work (Bureau of Labor Statistics, 2016). According to the European Labor Force Survey (LFS), in 1999, 4.1 million workers were subjected to WMSDs. In the same year, 3158 in every 100,000 workers in the construction sector suffered from WMSDs, and in 1292 cases, workers took 14 or more days of leave of absence from work (European Agency for Safety and Health at Work, 2010). According to the Liberty Mutual Workplace Safety Index, in 2009, WMSDs caused by overexertion resulted in $12.75 billion in workers' compensation costs which was 25.4% of all compensation costs (Liberty Mutual Research Institute For Safety, 2011). These and similar figures provide a glimpse into the loss of productivity at construction sites due to WMSDs. This has also intrigued researchers to explore ways to ergonomically prevent WMSD-related hazards.

According to the Occupational Safety and Health Administration (OSHA), there are eight risk factors related to WMSDs including force, repetition, awkward postures, static postures, quick motion, compression or contact stress, vibration, and extreme temperatures (OSHA, 2000). Most often, awkward postures can be prevented by rearranging the workplace or selecting proper tools for workers. But different jobs are associated with different types of risks and the challenge is to identify the correct ergonomic risks associated with a particular job. A thorough job hazards analysis (JHA) can identify the risks at the workplace, but it may be challenging to carry out the analysis because of complexity of the job and the manual effort needed to monitor work processes (Alwasel et al., 2011). Therefore, the objective of this paper is to present a methodology to facilitate the process of unobtrusively monitoring body postures of workers to autonomously assess and preempt potential risk factors.

## 2. Prevention through design (PTD) and risk assessment

Prevention through Design (PtD) is an initiative taken by the National Institute for Occupational Safety and Health (NIOSH). It encompasses a host of efforts to anticipate and design out ergonomic-related hazards in facilities, work methods, operations, processes, equipment, tools, products, new technologies, and the organization of work (NIOSH, 2014a). The goal of the PtD initiative is to prevent and control occupational injuries, illnesses, and fatalities. According to NIOSH, this goal can be achieved by: 1) eliminating or reducing potential risks to workers to an acceptable level at the source or as early as possible in a project life cycle, 2) including design, redesign, and retrofit of new and existing work premises, structures, tools, facilities, equipment, machinery, products, substances, work processes, and the organization of work, and 3) enhancing the work environment through enabling the prevention methods in all designs that affect workers and others on the premises.

A proper PtD practice requires prior identification of the risk factors on a jobsite which in turn, necessitates that work-related data be adequately collected, and subsequently used in an integrated risk assessment framework. In general, three different data collection approaches have been practiced for identifying risk factors: 1) self-assessment, where workers are asked to fill out a form to identify the risk levels associated with their tasks, 2) observation, where a job analyst assesses the risk factors by observing the jobsite in real time or via a recorded video, and 3) direct measurement, where instruments are used to measure postures directly (NIOSH, 2014b).

1. In the self-assessment approach, data are collected on both physical and psychosocial factors through interviews and questionnaires (David, 2005). This approach has relative advantages of having low initial cost, being straightforward to use and applicable to wide range of workplace situations (David, 2005). However, since a large number of samples are required to ensure that collected data are representative of the group of workers, subsequent costs for analysis and the required skills for interpreting the findings are generally high (David, 2005). Moreover, researchers have stated that workers' self-assessments on exposure level are often imprecise, unreliable, and biased (Viikari-Juntura et al., 1996; Balogh et al., 2004; Spielholz et al., 2001).
2. Observation-based approach is a simpler method that includes real-time assessment of exposure factors by systematic evaluation of the workers on the jobsite (Teschke et al., 2009). Despite being inexpensive and practical for a wide range of work situations, this method is disruptive in nature, and is subjected to intra- and inter-observer variability (David, 2005). An advanced method of observation-based assessment includes analyzing recorded video (Mathiassen et al., 2013; Dartt et al., 2009) which allows for more exposure factors to be obtained, but is mostly impractical due to the substantial cost, time, and technical knowledge required (David, 2005).
3. Unlike the previous two approaches, direct measurement uses tools attached to workers' bodies to collect data. Examples of this type of approach include but are not limited to using magneto-resistive angle sensors to measure shoulder flexion (Alwasel et al., 2011), Kinect or depth sensors to analyze posture by detecting position of skeleton joints at high sampling rates (Diego-Mas and Alcaide-Marzal, 2014; Plantard et al., 2015; Más et al., 2014), and smartphone's built-in accelerometer and gyroscope sensors to measure arm inclination (Yang, 2015). Previous work in this area has revealed that the direct measurement approach yields the most valid assessment of risk factors compared to other approaches (Kilbom, 1994; Winkel and Mathiassen, 1994). Building on previous work from multiple disciplines, in this research, a methodology is designed and validated to accurately identify a worker's body postures while carrying manual work. Ultimately, the findings of this research are sought to contribute to the PtD's mission by enabling construction researchers and decision-makers to design field activities to eliminate (or significantly reduces) work-related ergonomics issues for construction workers.

### 2.1. Risk assessment of construction tasks associated with awkward postures

For the purpose of identifying risks associated with awkward postures, generally, postures of different body parts (e.g. trunk, shoulder, and elbow) are measured in terms of degree of bent from the neutral posture. A neutral posture occurs when a worker needs minimum effort for standing (i.e. standing straight with his or her

arms down) or sitting, while all joints are aligned and there is minimal physical stress on bones, muscles, nerves, or tendons (Ergonomic-Plus, 2016). The larger the difference between the degree of bent from the neutral posture, the higher the risk of bodily injuries due to awkward posture. Researchers have shown that the degree of bent of different body parts can be partitioned into ranges to minimize observational errors (Kilbom, 1994; Lowe, 2004; Wyka et al., 2009). Fig. 1 shows how trunk flexion, trunk lateral bend, shoulder flexion, shoulder abduction, and elbow flexion are measured, by measuring the angle deviated from neutral posture, and Table 1 shows suggested posture categories (Andrews et al., 2012).

## 3. Research scope and objectives

As previously stated, sensor-based direct measurement of risk factors presents a great opportunity for precise and unobtrusive ergonomic assessment of construction tasks. Nevertheless, setting up, calibrating, and using a sophisticated sensor network requires expertise that is normally beyond what is expected from most construction workers and field practitioners. Even if such skills are available, the upfront investment as well as the time commitment necessary to purchase, install, and maintain the equipment may be considered a hindering factor (David, 2005). In previous studies, researchers achieved an RMS error of 3° while measuring the knee flexion/extension angles using Inertial Measurement Units (IMUs) (Seel et al., 2014). Other studies incorporated IMUs to measure multiple joint angles (Vignais et al., 2013) and gait stability (Jebelli et al., 2014). Since smartphone sensors are technically a class of IMUs, to overcome the implementation challenges, in this research smartphones are used as data collection devices. Moreover, smartphones have advantages of ubiquity, low procurement and maintenance cost, and ease of use. Additionally, smartphones are generally equipped with a large number of sensors (20 on average) that can be activated on demand to collect various modes of data. However, in this study, only one sensor (i.e. 3D accelerometer) is ultimately used to demonstrate the potential of mobile devices in ergonomic assessment. It should be noted that generally accelerometers in IMUs have higher sensitivity (i.e. range) than the smartphone's accelerometer, but for static postures, smartphone's built-in inertial sensors are reliable compared to other standard tools (Mourcou et al., 2015). Because in static postures, gravity acceleration dominates over body acceleration, 3D accelerometer can be used as inclinometer with the sensitivity of ± 1 g (Luinge and Veltink, 2005). Since most smartphones have higher sensitivity (e.g. ± 2 g) than the expected range (e.g. ± 1 g) for static postures, these devices can precisely capture data for static posture analysis.

The rest of this paper is organized as follows: The data collection and analysis methodology is described in detail in Sections 4 and 5. Next, Section 6 reports on the experiments carried out to test the hypothesis, and evaluate the practicality of using smartphones for ergonomics assessment of construction tasks. The developed scientific methodology is rooted in novel computing techniques. It contributes to the existing body of knowledge and practice by automating the process of ergonomics assessment without interrupting field activities. It also eliminates the need for extra training required to carry out data collection and analysis tasks.

## 4. Methodology

Fig. 2 shows the overall process that starts with sensory data collection. Details of this process are described in the following Subsections. In a nutshell, while a worker is performing a task, sensory data from two smartphones (as shown in Fig. 3), one mounted on the worker's upper-arm and another on the waist, are collected. The collected data are preprocessed for feature extraction and then the most distinctive features are selected for further analysis.

### 4.1. Data collection

Timestamped data are collected from three built-in smartphone sensors, namely accelerometer gyroscope, and linear accelerometer, in all three axes (i.e. X, Y, and Z). The accelerometer sensor measures the acceleration vector of the device and returns the components of the acceleration in three local Cartesian axes. The gyroscope sensor measures the rotation rate (i.e. angular velocity) of the device by measuring the roll, pitch, and yaw motions of the smartphone about the X, Y, and Z axes, respectively. Similar to accelerometer, the linear accelerometer sensor measures the acceleration of the device, but it excludes the gravity effect on the device. Fig. 4 shows the arrangement of the local Cartesian axes and the rotational angles.

### 4.2. Data preparation

Collected sensory data contains noise which should be removed before the data can be used for analysis. It is very common for a smartphone sensor to temporarily freeze and stop recording data during a relatively long period of recording. When the sensor recovers from freezing, it records data at a higher rate to compensate for missing data points. This essentially means that the resulting sensory data may not follow a uniform time series. Similar to past work (Akhavian and Behzadan, 2015; Akhavian et al., 2015), in this research, in order to have a continuous and orderly data stream, collected data are processed into 100 Hz of uniform time series by removing redundant data and interpolating missing data.

### 4.3. Feature extraction

Collecting raw data at a high sampling rate results in a significantly large number of data points that is computationally

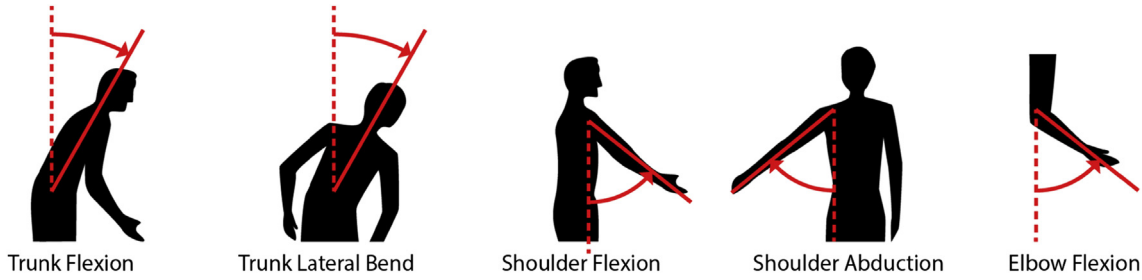


**Fig. 1.** Trunk flexion, trunk lateral bend, shoulder flexion, shoulder abduction, and elbow flexion.

**Table 1**
Suggested Category sizes for observation-based measurement of trunk flexion, trunk lateral bend, shoulder flexion, shoulder abduction, and elbow flexion.

| Ergonomic Risk | Trunk Flexion | Trunk Lateral Bend | Shoulder Flexion | Shoulder Abduction | Elbow Flexion |
|---|---|---|---|---|---|
| Low | 0°-30° | 0°-15° | 0°-30° | 0°-30° | 0°-30° |
| | 30°-60° | 15°-30° | 30°-60° | 30°-60° | 30°-60° |
| | 60°-90° | 30°-45° | 60°-90° | 60°-90° | 60°-90° |
| | > 90° | | 90°-120° | 90°-120° | > 90° |
| High | | | > 120° | > 120° | |

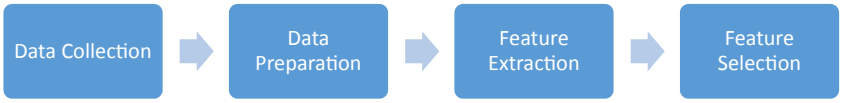


**Fig. 2.** Schematic diagram of overall data processing.

**Fig. 3.** Smartphones mounted on the Worker's upper-arm and waist.

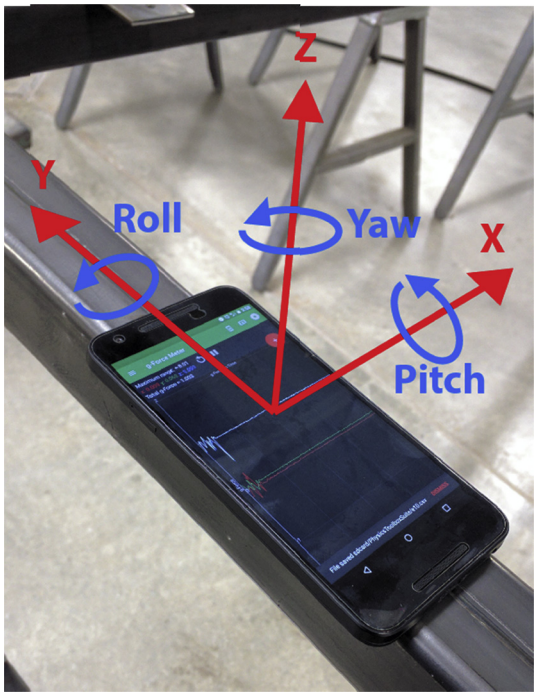


**Fig. 4.** Local cartesian axes and rotational angles in a smartphone.

inefficient to handle. To address this issue, raw time series data needs to be compressed by being segmented into several windows for feature extraction (Khan et al., 2011). In this study, raw data are segmented into 2-s windows (each containing 200 data points) with 50% overlay. Previous research in this area has indicated that data segmentation by overlapping adjacent windows reduces the errors caused by transition state noise (Su et al., 2014). Finally, statistical time-domain features (e.g. mean, maximum, minimum, and interquartile range (IQR)), as shown in Fig. 5, are calculated for each window since time-domain features are most commonly used in data mining for activity recognition using smartphones (Shoaib et al., 2015).

### 4.4. Feature selection

Not all extracted features are useful since not all yield distinguishable patterns. For example, it may turn out that the mean of the windows in the X axis does not contain value-adding information and thus can be excluded from computations. In order to identify the most effective features (a.k.a. distinctive features), two feature selection algorithms, namely Correlation-based Feature Selection (CFS) and ReliefF are applied to the dataset. By definition, CFS is an algorithm that uses a correlation-based approach and heuristic search strategy to find the best feature sets containing features that are highly correlated with the classes, yet uncorrelated to each other (Hall, 1999). ReliefF is a feature selection algorithm that assigns weights to the features and ranks them according to how well their values distinguish between neighboring instances of same and different classes (Yu and Liu, 2003).

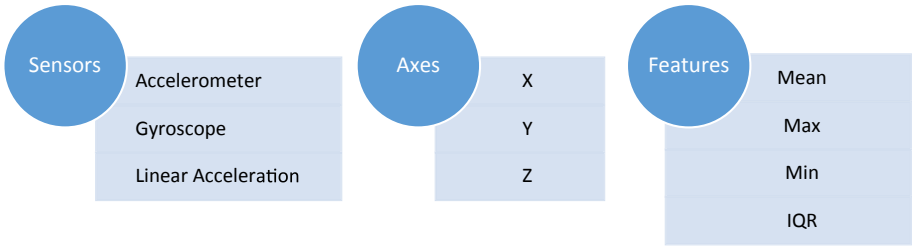


**Fig. 5.** Extracted features for data analysis.

Using CFS, first, irrelevant and redundant features are removed, and then the remaining features are ranked using ReliefF. Finally, the best 9 features out of a total of 36 (i.e. 4 features in 3 axes from 3 sensors) are selected for further analysis. Using these algorithms, it was found that the accelerometer sensor's mean, maximum, and minimum features (for all three axes) are the best features for this study. Fig. 6 summarizes the selected features for data analysis in this research.

## 5. Analysis of human postures using wearable smartphones

In this Section, a worker's postures while performing a manual screw driving task are analyzed using data from bodily-mounted smartphone sensors. First, the mathematical description of the hypothesis established to measure the worker's trunk and shoulder flexions from the smartphone's accelerometer sensor is presented. Next, predicted postures from data are compared with observation-based measurements to evaluate the accuracy of the developed methods.

### 5.1. Hypothesis

In general, for ergonomic posture analysis, body postures are determined by angular rotations of different body parts (e.g. trunk flexion, trunk lateral bend, shoulder flexion, shoulder abduction, elbow flexion, neck bent, neck twist, wrist bent, forearm twist, knee angle, ankle posture) (NIOSH, 2014b; OSHA, 2011). In this research, a body posture is defined as a vector that consists of angular rotations of $m$ different body parts, as shown in Equation (1),

$$\mathrm{T}_i = \begin{bmatrix} \beta_{i1} \\ \beta_{i2} \\ \beta_{i3} \\ \cdots \\ \beta_{im} \end{bmatrix} \tag{1}$$

where $\beta_{im}$ is the angular rotation of body part $m$ in posture vector $T_i$. For example, a posture vector $T_1$, consisting of five components, namely trunk flexion (TF), trunk lateral bend (TLB), shoulder flexion (SF), shoulder abduction (SA), and elbow flexion (EF), can be shown as in Equation (2),

$$T_1 = \begin{bmatrix} TF1 \\ TLB_1 \\ SF_1 \\ SF_1 \\ SA_1 \end{bmatrix} \tag{2}$$

Using the definition in Equation (1), the neutral posture ($T_0$) can be expressed as a null vector. As a convention, feature $k$ corresponding to a posture $T$ is shown as $T \cdot feature_k$. It is important to normalize features prior to further processing. Feature normalization can be done by subtracting features obtained from the neutral posture from the corresponding features obtained from posture $T$. A normalized feature is denoted as $T \cdot feature'_k$ and mathematically expressed by Equation (3),

$$Ti \cdot feature'_k = T_i \cdot feature_k - T_0 \cdot feature_k \tag{3}$$

It is thus imperative that the normalized feature vector for the neutral posture be a null (i.e. a zero) vector. Finally, as described in Subsection 4.4, in this research, the feature space is defined by Equation (4), below,

$$Feature\ space = \left\{ \begin{matrix} Accelerometer\_X\_Avg, Accelerometer\_X\_Max, Accelerometer\_X\_Min, \\ Accelerometer\_Y\_Avg, Accelerometer\_Y\_Max, Accelerometer\_Y\_Min, \\ Accelerometer\_Z\_Avg, Accelerometer\_Z\_Max, Accelerometer\_Z\_Min \end{matrix} \right\} \tag{4}$$

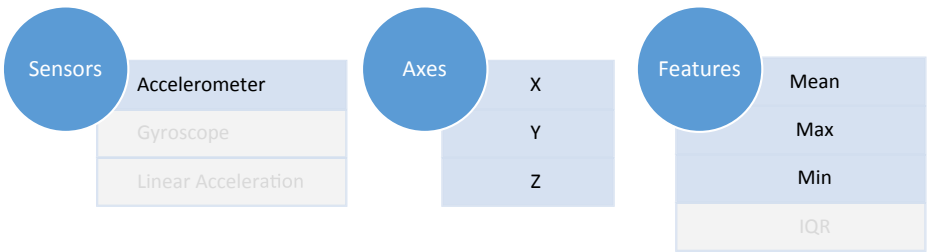


**Fig. 6.** Selected features for data analysis.

For example, $T_1 \cdot Accelerometer\_X\_Avg'$ refers to the normalized mean of the accelerometer data about the X axis while the worker was in posture $T_1$.Using this convention, if a posture $S$ can be expressed as the weighted sum of $n$ base postures ($T_1$, $T_2$, $T_3$, …, $T_n$), as shown in Equation (5) (referred to as posture composition equation) then it is hypothesized that a normalized feature $k$ obtained from sensory data while the worker is in posture $S$ can be expressed as the weighted sum of that same normalized feature $k$ obtained from sensory data corresponding to base postures $T_1$, $T_2$, $T_3$, …, $T_n$, as formulated in Equations (5) and (6) (referred to as feature composition equation). Further, the weight of each feature of a base posture, $f(\alpha_i)$ in the feature composition equation is a function of the corresponding weight of the same base postures, $\alpha_i$ in the posture composition equation. In mathematical terms, if,

$$S = \alpha_1 T_1 + \alpha_2 T_2 + \alpha_3 T_3 + \ldots + \alpha_n T_n = \sum_{i=1}^{n} \alpha_i T_i \tag{5}$$

then,

$$\begin{aligned} S \cdot feature'_k &= f(\alpha_1) T_1 \cdot feature'_k + f(\alpha_2) T_2 \cdot feature'_k \\ &\quad + f(\alpha_3) T_3 \cdot feature'_k + \ldots + f(\alpha_n) T_n \cdot feature'_k \\ &= \sum_{i=1}^{n} f(\alpha_i) T_i \cdot feature'_k \end{aligned} \tag{6}$$

### 5.2. Mathematical analysis of the hypothesis

In this Subsection, several corollary propositions are developed, based on the hypothesis described in Subsection 5.1, which are further used to discover the relationship between the posture vector and the extracted features. Assume a general posture vector $T_i$ consists of $m$ number of components, denoted with $\beta$ which is mathematically expressed by Equation (1). Then, from Equation (5), any given posture $S$ can be written as,

$$\begin{aligned} S &= \alpha_1 T_1 + \alpha_2 T_2 + \ldots + \alpha_n T_n \\ &= \alpha_1 \begin{bmatrix} \beta_{11} \\ \beta_{12} \\ \beta_{13} \\ \ldots \\ \beta_{1m} \end{bmatrix} + \alpha_2 \begin{bmatrix} \beta_{21} \\ \beta_{22} \\ \beta_{23} \\ \ldots \\ \beta_{2m} \end{bmatrix} + \ldots + \alpha_n \begin{bmatrix} \beta_{n1} \\ \beta_{n2} \\ \beta_{n3} \\ \ldots \\ \beta_{nm} \end{bmatrix} \\ &= \begin{bmatrix} \alpha_1 \\ \alpha_2 \\ \alpha_3 \\ \ldots \\ \alpha_m \end{bmatrix} \begin{bmatrix} \beta_{11} & \beta_{21} & \beta_{31} & \ldots & \beta_{m1} \\ \beta_{12} & \beta_{22} & \beta_{32} & \ldots & \beta_{m2} \\ \beta_{13} & \beta_{23} & \beta_{33} & \ldots & \beta_{m3} \\ \ldots & \ldots & \ldots & \ldots & \ldots \\ \beta_{1m} & \beta_{2m} & \beta_{3m} & \ldots & \beta_{mm} \end{bmatrix} \end{aligned} \tag{7}$$

According to Equation (7), posture $S$ can be expressed as the sum of weighted $n$ base postures $T$, using $n$ unknown multipliers ($\alpha_1$, $\alpha_2$, $\alpha_3$, …, $\alpha_n$) and $m$ independent equations. If $n = m$, then the number of unknowns will be equal to the number of independent equations. Hence, Equation (7) can be solved mathematically to find the unknown values of multipliers, i.e., in matrix form: $S = \alpha \cdot T \Rightarrow \alpha = T^{-1} \cdot S$

Assume that an arbitrary posture $S$ is identical to any given base posture $T_i$. Therefore, from Equation (5), $\alpha_i = 1$, and $\alpha_j = 0$ for all $j \neq i$. In this case, features of posture S are identical to features of base posture $T_i$, and thus, from Equation (6), $f(\alpha_i) = 1$, and $f(\alpha_j) = 0$ for all $j \neq i$. This important observation serves as the basis for establishing key boundary conditions when attempting to find a mathematical relationship between $\alpha$ values and corresponding $f(\alpha)$ values.

From the two boundary conditions, it can be inferred that the mathematical function $f(\alpha)$ can be any of the three types; algebraic, polynomial, or trigonometric, which can be expressed in the general forms of $f(\alpha) = \alpha$, $f(\alpha) = \alpha^m$, and $f(\alpha) = \sin(90\alpha)$, respectively.

All features, either of combined posture ($S$) or of any base posture ($T_i$), should be normalized to satisfy both boundary conditions. As stated earlier, normalization is done by subtracting the feature of the neutral posture from the corresponding feature obtained from any given posture.

## 6. Validation experiments

As mentioned in Section 4, for posture analysis of the manual screw driving task, two smartphones were mounted on a worker's body, one on the upper-arm and another on the waist. Previous research has shown that these two positions produce the most distinctive features for most manual jobs performed by field workers (Joshua and Varghese, 2011; Yang and Hsu, 2010). As shown in Fig. 7, data were collected from both smartphones for six base body postures. Collected data were then preprocessed and features were extracted. In particular, data collected from the smartphone on the upper arm were used for measuring total flexion (combined effect of trunk and shoulder flexions), while data collected from the smartphone on the waist was used to measure trunk flexion. For the specific task of screw driving, as shown in the postures of Fig. 7, trunk flexion involves downward angular movements while shoulder flexion involves upward angular movements. Therefore, the total flexion is measured by subtracting


**Fig. 7.** Six base postures for the screw driving experiment.

**Table 2**
Observed values for Trunk, Shoulder and Total Flexions of Six Postures.

| Postures | $P_1$ | $P_2$ | $P_3$ | $P_4$ | $P_5$ | $P_6$ |
|---|---|---|---|---|---|---|
| Trunk Flexion (°) | 0 | 0 | 0 | 0 | 30 | 90 |
| Shoulder Flexion (°) | 0 | 90 | 120 | 30 | 60 | 90 |
| Total Flexion (°) | 0 | 90 | 120 | 30 | 30 | 0 |

the trunk flexion from the shoulder flexion. Finally, by combining the results from both smartphones, values for trunk flexion and shoulder flexion were determined individually. Referring to the six postures shown in Fig. 7, trunk, shoulder, and total flexions are tabulated in Table 2.

Since all angles are zero for posture $P_1$, this posture is considered as the neutral posture (i.e. $T_0 = P_1$). As previously discussed, the number of base postures should be selected as equal to the number of components of a posture vector. In this experiment, each posture vector consists of a single component, which is total flexion for the upper arm-mounted smartphone and trunk flexion for the waist-mounted smartphone. Therefore, one base posture must be selected for analysis in each case. Here, posture $P_2$ is selected for the upper arm-mounted smartphone, and posture $P_6$ is selected for the waist-mounted smartphone. Since, $P_2$ and $P_6$ both represent an angular vector of 90°, Equation (5) can be rewritten as $P_i = \alpha \cdot 90°$. Equation (6) can be rewritten as,

$$P_i \cdot feature_k = f(\alpha)[P_{90} \cdot feature_k - P_1 \cdot feature_k] + P_1 \cdot feature_k \quad (8)$$

where, $P_{90} = P_2$ and $i = 3, 4, 5, 6$ for the upper arm-mounted smartphone, and $P_{90} = P_6$ and $i = 2, 3, 4, 5$ for the waist-mounted smartphone.

### 6.1. Developing a general equation for $P_i \cdot feature_k$

Investigation of extracted features reveals that a trigonometric relationship between $\alpha$ and $f(\alpha)$ yields the most accurate prediction of $P_i \cdot feature_k$. Further investigation reveals that the best trigonometric relation is a sine function for the features (i.e. mean, maximum, and minimum) extracted from accelerometer-X and accelerometer-Z sensors, and a cosine function for the features extracted from accelerometer-Y sensors.

Considering a general form of sine function, i.e., $f(\alpha) = a^*\sin(90\alpha) + c$, and applying two boundary conditions, we get $a = 1$ and $c = 0$. Hence, Equation (8) can be rewritten as,

$$P_i \cdot feature_k = \sin(90\alpha)[P_{90} \cdot feature_k - P_1 \cdot feature_k] + P_1 \cdot feature_k \quad (9)$$

Similarly, considering a general form of cosine function, i.e., $f(\alpha) = a^*\cos(90\alpha) + c$, and applying two boundary conditions, we get $a = -1$ and $c = 1$. Hence, Equation (8) can be rewritten as,

$$P_i \cdot feature_k = \cos(90\alpha)[P_1 \cdot feature_k - P_{90} \cdot feature_k] + P_{90} \cdot feature_k \quad (10)$$

### 6.2. Prediction of $P_i \cdot feature_k$

Using Equations (9) and (10), features from each posture can be calculated and compared to the features obtained by analyzing smartphones' sensory data. Results are shown in Tables 3 and 4. In these Tables, the *Experimental Result* column shows the values of extracted features from the actual sensory data, while the values in the *Obtained Result* column show the predicted features using Equations (9) and (10). For each posture, minimum absolute errors are highlighted in Tables 3 and 4. Table 3 shows that, for all four postures, *Accelerometer-Y-Max* features are predicted with the least error compared to other features. Table 4 also shows that *Accelerometer-Y-Avg* and *Accelerometer-Y-Max* are predicted with least error compared to other features. For both cases (i.e. for the upper arm-mounted smartphone which measures the total flexion, and for waist-mounted smartphone which measures the trunk flexion), predictions for *Accelerometer-Y-Max* features, using Equations (9) and (10) are the most accurate compared to other features. Therefore, it can be concluded that prediction of total and trunk flexion from the *Accelerometer-Y-Max* data will yield the most accurate results.

### 6.3. Developing an equation for finding $P_i$ from $P_i \cdot feature_k$

Since the *Accelerometer-Y-Max* feature is the most reliable feature for predicting $P_i$, as established in previous Subsection, substituting $P_i = \alpha.90°$ and $feature_k$ = *Accelerometer_Y_Max*, Equation (10) can be rewritten as,

$$P_i = cos^{-1}\left(\frac{P_i \cdot Accelerometer\_Y\_Max - P_{90} \cdot Accelerometer\_Y\_Max}{P_1 \cdot Accelerometer\_Y\_Max - P_{90} \cdot Accelerometer\_Y\_Max}\right) \quad (11)$$

where, for the upper arm-mounted smartphone, $P_i$ = total flexion, $P_{90} = P_2$, and $i = 3, 4, 5, 6$, and for the waist-mounted smartphone, $P_i$ = trunk flexion, $P_{90} = P_6$, and $i = 2, 3, 4, 5$.

### 6.4. Prediction of $P_i$

Using Equation (11) and sensory data from the upper arm-mounted smartphone, total flexions are measured for four postures and tabulated in Table 5. Similarly, trunk flexions are measured using Equation (11) and sensory data from the waist-

**Table 3**
Comparison of results for upper-arm-mounted smartphone.

| Sensor/Posture | | Experimental result | | | | Obtained result | | | | Error | | | |
|---|---|---|---|---|---|---|---|---|---|---|---|---|---|
| | | $P_3$ | $P_4$ | $P_5$ | $P_6$ | $P_3$ | $P_4$ | $P_5$ | $P_6$ | $P_3$ | $P_4$ | $P_5$ | $P_6$ |
| Acc.X | Avg | −0.803 | −0.576 | −0.479 | −0.214 | −0.668 | −0.332 | −0.332 | −0.164 | 17% | 42% | 31% | 23% |
| | Min | −0.764 | −0.549 | −0.446 | −0.175 | −0.707 | −0.46 | −0.46 | −0.123 | 7% | 16% | −3% | 29% |
| | Max | −0.846 | −0.613 | −0.514 | −0.251 | −0.783 | −0.538 | −0.538 | −0.204 | 7% | 12% | −5% | 19% |
| Acc.Y | Avg | 0.3617 | −0.787 | −0.849 | −0.942 | 0.3752 | −0.835 | −0.835 | −0.953 | −4% | −6% | 2% | −1% |
| | Min | 0.3849 | −0.768 | −0.831 | −0.919 | 0.4066 | −0.816 | −0.816 | −0.936 | −6% | −6% | 2% | −2% |
| | Max | 0.3375 | −0.806 | −0.868 | −0.965 | 0.3418 | −0.854 | −0.854 | −0.971 | −1% | −6% | 2% | −1% |
| Acc.Z | Avg | 0.5245 | 0.0909 | 0.0119 | −0.056 | 0.4893 | 0.2912 | 0.2912 | 0.0207 | 7% | −220% | −2345% | 137% |
| | Min | 0.5549 | 0.1202 | 0.0463 | −0.02 | 0.5181 | 0.3213 | 0.3213 | 0.0524 | 7% | −167% | −594% | 359% |
| | Max | 0.4951 | 0.0624 | −0.016 | −0.094 | 0.46 | 0.2603 | 0.2603 | −0.013 | 7% | −317% | 1703% | 87% |

**Table 4**
Comparison of results for waist-mounted smartphone.

| Sensor/Posture | | Experimental Result | | | | Obtained Result | | | | Percent Error | | | |
|---|---|---|---|---|---|---|---|---|---|---|---|---|---|
| | | $P_2$ | $P_3$ | $P_4$ | $P_5$ | $P_2$ | $P_3$ | $P_4$ | $P_5$ | $P_2$ | $P_3$ | $P_4$ | $P_5$ |
| Acc.X | Avg | −0.208 | −0.214 | −0.203 | −0.454 | −0.171 | −0.171 | −0.171 | −0.498 | 18% | 20% | 16% | −10% |
| | Min | −0.198 | −0.205 | −0.194 | −0.445 | −0.161 | −0.161 | −0.161 | −0.486 | 19% | 21% | 17% | −9% |
| | Max | −0.22 | −0.225 | −0.213 | −0.463 | −0.183 | −0.183 | −0.183 | −0.511 | 17% | 19% | 14% | −10% |
| Acc.Y | Avg | 1.0168 | 1.0287 | 1.0258 | 0.9526 | 1.0239 | 1.0239 | 1.0239 | 0.9665 | −1% | 0% | 0% | −1% |
| | Min | 1.0254 | 1.0375 | 1.0336 | 0.9593 | 1.0311 | 1.0311 | 1.0311 | 0.9738 | −1% | 1% | 0% | −2% |
| | Max | 1.0084 | 1.0195 | 1.0184 | 0.9462 | 1.0163 | 1.0163 | 1.0163 | 0.9587 | −1% | 0% | 0% | −1% |
| Acc.Z | Avg | 0.2113 | 0.1154 | 0.1697 | 0.043 | 0.219 | 0.219 | 0.219 | 0.0165 | −4% | −90% | −29% | 62% |
| | Min | 0.2175 | 0.1247 | 0.1765 | 0.0514 | 0.2253 | 0.2253 | 0.2253 | 0.0256 | −4% | −81% | −28% | 50% |
| | Max | 0.2049 | 0.1073 | 0.1632 | 0.0348 | 0.212 | 0.212 | 0.212 | 0.0062 | −3% | −97% | −30% | 82% |

**Table 5**
Prediction of total flexions.

| Postures | P1.Accelerometer_Y_Max | P90.Accelerometer_Y_Max | Pi.Accelerometer_Y_Max | Total flexion, $P_i$ (°) |
|---|---|---|---|---|
| $P_3$ | −0.971371297 | −0.095891187 | 0.337469734 | 120 |
| $P_4$ | −0.971371297 | −0.095891187 | −0.806222257 | 36 |
| $P_5$ | −0.971371297 | −0.095891187 | −0.867731428 | 28 |
| $P_6$ | −0.971371297 | −0.095891187 | −0.965261204 | 7 |

**Table 6**
Prediction of trunk flexions.

| Postures | P1.Accelerometer_Y_Max | P90.Accelerometer_Y_Max | Pi.Accelerometer_Y_Max | Trunk flexion, $P_i$ (°) |
|---|---|---|---|---|
| $P_2$ | 1.016270039 | 0.586581745 | 1.008369841 | 11 |
| $P_3$ | 1.016270039 | 0.586581745 | 1.019543369 | 0 |
| $P_4$ | 1.016270039 | 0.586581745 | 1.018436005 | 0 |
| $P_5$ | 1.016270039 | 0.586581745 | 0.946233972 | 33 |


**Fig. 8.** Ten new postures for the screw driving experiment.

**Table 7**
Prediction of total flexions of new arbitrary postures.

| Posture | $P_1$.Accelerometer_Y_Max | $P_{90}$.Accelerometer_Y_Max | $P_i$.Accelerometer_Y_Max | Total flexion, $P_i$ (°) |
|---|---|---|---|---|
| $P_7$ | −0.93446 | −0.07067 | −0.6867 | 45 |
| $P_8$ | −0.93446 | −0.07067 | −0.93205 | 4 |
| $P_9$ | −0.93446 | −0.07067 | −0.60958 | 51 |
| $P_{10}$ | −0.93446 | −0.07067 | −0.14265 | 85 |
| $P_{11}$ | −0.93446 | −0.07067 | −0.93446 | 0 |
| $P_{12}$ | −0.93446 | −0.07067 | −0.57244 | 54 |
| $P_{13}$ | −0.93446 | −0.07067 | −0.18295 | 83 |
| $P_{14}$ | −0.93446 | −0.07067 | −0.07067 | 90 |
| $P_{15}$ | −0.93446 | −0.07067 | −0.56386 | 55 |
| $P_{16}$ | −0.93446 | −0.07067 | −0.36909 | 70 |

**Table 8**
Prediction of trunk flexions of new arbitrary postures.

| Posture | $P_1$.Accelerometer_Y_Max | $P_{90}$.Accelerometer_Y_Max | $P_i$.Accelerometer_Y_Max | Trunk flexion, $P_i$ (°) |
|---|---|---|---|---|
| $P_7$ | 1.041574 | 0.879573 | 1.041574 | 45 |
| $P_8$ | 1.041574 | 0.879573 | 1.015564 | 37 |
| $P_9$ | 1.041574 | 0.879573 | 1.018172 | 83 |
| $P_{10}$ | 1.041574 | 0.879573 | 1.000776 | 127 |
| $P_{11}$ | 1.041574 | 0.879573 | 1.022249 | 28 |
| $P_{12}$ | 1.041574 | 0.879573 | 0.999042 | 97 |
| $P_{13}$ | 1.041574 | 0.879573 | 0.994996 | 127 |
| $P_{14}$ | 1.041574 | 0.879573 | 1.016283 | 122 |
| $P_{15}$ | 1.041574 | 0.879573 | 1.017257 | 87 |
| $P_{16}$ | 1.041574 | 0.879573 | 0.879573 | 160 |

**Table 9**
Predicted vs. Observed Measurements of Trunk Flexion (TF) and Shoulder Flexion (SF).

| Posture | Predicted | | Observed | | Difference = Observed - Predicted | |
|---|---|---|---|---|---|---|
| | TF | SF | TF | SF | TF | SF |
| $P_3$ | 0 | 120 | 0 | 120 | 0 | 0 |
| $P_4$ | 0 | 36 | 0 | 30 | 0 | −6 |
| $P_5$ | 33 | 61 | 30 | 60 | −3 | −1 |

**Table 10**
Predicted vs. Observed Measurements of Arbitrary Postures.

| Posture | Predicted | | Observed | | Difference = Observed - Predicted | |
|---|---|---|---|---|---|---|
| | TF | SF | TF | SF | TF | SF |
| $P_7$ | 0 | 45 | 0 | 45 | 0 | 0 |
| $P_8$ | 33 | 37 | 40 | 40 | 7 | 3 |
| $P_9$ | 31 | 83 | 30 | 85 | −1 | 2 |
| $P_{10}$ | 42 | 127 | 35 | 130 | −7 | 3 |
| $P_{11}$ | 28 | 28 | 45 | 40 | 17 | 12 |
| $P_{12}$ | 42 | 97 | 40 | 100 | −2 | 3 |
| $P_{13}$ | 45 | 127 | 45 | 125 | 0 | −2 |
| $P_{14}$ | 32 | 122 | 25 | 115 | −7 | −7 |
| $P_{15}$ | 32 | 87 | 25 | 90 | −7 | 3 |
| $P_{16}$ | 90 | 160 | 90 | 160 | 0 | 0 |

mounted smartphone, and listed in Table 6.

In addition to the six initial postures ($P_1$ through $P_6$) explained throughout the paper, more experiments were conducted to further assess the robustness and accuracy of the developed formulation in predicting arbitrary body postures of workers involved in manual tasks. In particular, 10 new body postures ($P_7$ through $P_{16}$), shown in Fig. 8, were analyzed. It should be noted that these 16 body postures were randomly selected to cover all risk categories (ranging from low, to medium, to high) as described in Table 1. Tables 7 and 8 show calculations of total and trunk flexions of these body postures, respectively.

### 6.5. Analysis of results

Shoulder flexion (SF) is measured by subtracting trunk flexion (TF) from the total flexion. Predicted values for TF and SF for postures $P_3$, $P_4$ and $P_5$, along with the observation-based measurements are tabulated in Table 9. Similarly, in Table 10, predicted values for TF and SF for the 10 arbitrary body postures ($P_7$ through $P_{16}$), along with the observation-based measurements are

**Table 11**
Risk Level of the Postures (H: high, M: medium, L: low).

| Postures | Flexions | | | | Risk Score | | | | | | Risk Level | |
|---|---|---|---|---|---|---|---|---|---|---|---|---|
| | Predicted | | Observed | | Predicted | | | Observed | | | Predicted | Observed |
| | TF | SF | TF | SF | TF | SF | TF+SF | TF | SF | TF+SF | | |
| *P1* | 0 | 0 | 0 | 0 | 1 | 1 | 2 | 1 | 1 | 2 | L | L |
| *P2* | 0 | 90 | 0 | 90 | 1 | 4 | 5 | 1 | 4 | 5 | M | M |
| *P3* | 0 | 120 | 0 | 120 | 1 | 4 | 5 | 1 | 4 | 5 | M | M |
| *P4* | 0 | 36 | 0 | 30 | 1 | 2 | 3 | 1 | 2 | 3 | L | L |
| *P5* | 33 | 61 | 30 | 60 | 2 | 3 | 5 | 2 | 3 | 5 | M | M |
| *P6* | 90 | 90 | 90 | 90 | 3 | 4 | 7 | 3 | 4 | 7 | H | H |
| *P7* | 0 | 45 | 0 | 45 | 1 | 2 | 3 | 1 | 2 | 3 | L | L |
| *P8* | 33 | 37 | 40 | 40 | 2 | 2 | 4 | 2 | 2 | 4 | M | M |
| *P9* | 31 | 83 | 30 | 85 | 2 | 3 | 5 | 2 | 3 | 5 | M | M |
| *P10* | 42 | 127 | 35 | 130 | 2 | 5 | 7 | 2 | 5 | 7 | H | H |
| *P11* | 28 | 28 | 45 | 40 | 1 | 1 | 2 | 2 | 2 | 4 | L | M |
| *P12* | 42 | 97 | 40 | 100 | 2 | 4 | 6 | 2 | 4 | 6 | M | M |
| *P13* | 45 | 127 | 45 | 125 | 2 | 5 | 7 | 2 | 5 | 7 | H | H |
| *P14* | 32 | 122 | 25 | 115 | 2 | 5 | 7 | 1 | 4 | 5 | H | M |
| *P15* | 32 | 87 | 25 | 90 | 2 | 3 | 5 | 1 | 4 | 5 | M | M |
| *P16* | 90 | 160 | 90 | 160 | 3 | 5 | 8 | 3 | 5 | 8 | H | H |

tabulated. It should be noted that the observation-based measurements were taken by visually inspecting the photos of each experiment, while the predicted (hypothesis-based) measurements were calculated using the methodology laid out in this paper.

## 7. Discussion

As listed in Tables 9 and 10, with a few exceptions, values calculated from the hypothesis are very close to the observation-based measurements. In particular, for posture $P_3$, $P_5$, $P_7$, $P_9$, $P_{12}$, $P_{13}$, and $P_{16}$ measurements of trunk and shoulder flexions by both approaches are either identical or within $\pm 3^\circ$ of the true values. For some postures such as $P_{11}$, $P_{14}$, and $P_{15}$, the difference between predicted and true values is slightly higher. Overall, it is very promising to observe that out of the 13 body postures tabulated in Tables 9 and 10, the absolute difference in TF and SF is $\leq 7^\circ$ in 12 postures. There is only one posture ($P_{11}$) for which the difference for both TF and SF is more than 7°. Further inspection of the experiment photos showed that the main reason behind this relatively large error was that the waist-mounted smartphone was not properly secured in this isolated body posture, and as a result, its orientation did not reflect the actual trunk flexion. Nonetheless, results shown in Tables 9 and 10 are all indicative that the predicted and observed TF and SF values for each body posture are either in the same ergonomic risk level or within one level from each other (as defined in Table 1), which implies that the developed methodology is a reliable tool for ergonomic risk analysis of manual construction tasks.

Table 11 shows the ergonomic risk level of each posture. For the TF of each posture, a risk score, ranging from 1 to 4 is given based on the value falling into the category size described in Table 1. Similarly, for SF, a risk score, ranging from 1 to 5 is given. The total risk score for each posture is then calculated by adding risk scores for TF and SF, resulting in the lowest possible score of 2 and the highest possible score of 9. The risk level of low (L), medium (M) or high (H) is assigned to each posture based on the total risk score being 2 to 3, 4 to 6, and 7 to 9, respectively. Table 11 shows that for 14 out of the 16 postures, risk levels calculated from the hypothesis and observation-based measurements are identical. As shown in this Table, for the specific screw driving task conducted in the validation experiment, postures $P_6$, $P_{10}$, $P_{13}$, $P_{14}$, and $P_{16}$ exposed the worker to a high level of ergonomic risk.

## 8. Summary and conclusions

Construction works are very labor-intensive and often stipulate the workers to go beyond their natural physical limits to cope up with the increasing complexities and challenges of their assigned tasks. Consequently, workers in this industry are more exposed to WMSDs which can translate into significant amounts of loss in project financial and human resources and negatively impact productivity. To prevent WMSDs, health and safety organizations have been emphasizing the need to identify hazardous jobsite risks and then ergonomically design the job so that it fits to the workers. An example of such initiative is PtD, taken by NIOSH, to prevent work-related injuries and fatalities by ergonomically designing the work environment. One of the goals of PtD is to identify and eliminate the ergonomic risks at the source and as early as possible. To identify risk levels on a jobsite, self-assessment, observation-based, or instrument-based direct measurement techniques can be used. Previous research has found that direct assessment is more accurate but often requires prior technical knowledge and investment. To overcome these implementation challenges, in this research smartphone sensors were used as measurement tools due to their ubiquity, low procurement and maintenance cost, and ease of use.

Since awkward posture is one of the eight major causes of WMSDs, the research primarily focused on assessing the risk levels associated with awkward postures while performing manual tasks. Generally, assessment of an awkward posture consists of measuring deviation angles of various body-parts, however, the presented research specifically focused on only trunk and shoulder flexions of the workers. In particular, it was hypothesized that if a composite posture could be defined as a weighted composition of base postures, then any feature of that posture would also be a weighted composition of the same corresponding features of the base postures. Furthermore, the weight factors in the feature composition will be functions of corresponding weights for the posture composition. Based on this hypothesis, an equation was developed to measure the components of posture vector from the features of that posture. In other words, an equation to measure trunk and shoulder flexions from the smartphone's sensory data was developed.

For validation of the developed hypothesis, experiment were performed with two smartphones mounted on a worker's body; one on the upper-hand and another on the waist. Data from the smartphones' sensors were collected while the worker was

performing a typical construction task, which was screw driving in this case. Collected data were preprocessed for feature extraction and the 9 most distinctive features were selected for further analysis. It was revealed that for the specific experiment designed and carried out in this research, the *Accelerometer_Y_Max* feature was the best feature for predicting measurement of the flexions. Therefore, the *Accelerometer_Y_Max* feature was chosen to measure the trunk and shoulder flexions and it was found that the predicted results based on the hypothesis were in very close agreement with the observation-based measurements, and could be reliably used to assess the level of ergonomic risk associated with the manual task conducted by the worker.

It must be noted that although the presented results in this paper primarily focused on posture analysis for trunk and shoulder flexions in a manual screw driving task, the developed methodology and analysis techniques can be generalized with minimum modifications to other types of field activities. Moreover, the proposed method is applicable for workers in various occupations who are exposed to WMSDs due to awkward postures. Examples include, but are not limited to industry laborers, carpenters, welders, farmers, health assistants, teachers, and office workers.

## Acknowledgement

The presented work has been supported by the U.S. National Science Foundation (NSF) through grant CMMI 1602236. The authors gratefully acknowledge the support from the NSF. Any opinions, findings, conclusions, and recommendations expressed in this paper are those of the authors and do not necessarily represent those of the NSF.

## References

Akhavian, R., Behzadan, A., 2015. Wearable sensor-based activity recognition for data-driven simulation of construction workers' activities. Huntington Beach, CA. In: Proceedings of the 2015 Winter Simulation Conference.

Akhavian, R., Brito, L., Behzadan, A., 2015. Integrated mobile sensor-based activity recognition of construction equipment and human crews. Ames, IA. In: Proceedings of the Conference on Autonomous and Robotic Construction of Infrastructure.

Alwasel, A., Elrayes, K., Abdel-Rahman, E.M., Haas, C., 2011. Sensing construction work-related musculoskeletal disorders (WMSDs). Seoul, Korea. In: Proceedings of the 28th International Symposium on Automation and Robotics in Construction.

Andrews, D.M., Fiedler, K.M., Weir, P.L., Callaghan, J.P., 2012. The effect of posture category salience on decision times and errors when using observation-based posture assessment methods. Ergonomics 55 (12), 1548–1558.

Balogh, I., Ørbæk, P., Ohlsson, K., Nordander, C., Unge, J., Winkel, J., Hansson, G.-Å., Group, M.S.S., 2004. Self-assessed and directly measured occupational physical activities—influence of musculoskeletal complaints, age and gender. Appl. Ergon. 35 (1), 49–56.

Bureau of Labor Statistics, 2014. Nonfatal Occupational Injuries and Illnesses Requiring Days Away from Work. U.S. Department of Labor. https://www.bls.gov/bls/newsrels.htm (Accessed November 2016).

Bureau of Labor Statistics, 2016. Nonfatal Occupational Injuries and Illnesses Requiring Days Away from Work. U.S. Department of Labor. https://www.bls.gov/news.release/pdf/osh2.pdf (Accessed February 2017).

Dartt, A., Rosecrance, J., Gerr, F., Chen, P., Anton, D., Merlino, L., 2009. Reliability of assessing upper limb postures among workers performing manufacturing tasks. Appl. Ergon. 40 (3), 371–378.

David, G.C., 2005. Ergonomic methods for assessing exposure to risk factors for work-related musculoskeletal disorders. Occup. Med. 55 (3), 190–199.

Diego-Mas, J.A., Alcaide-Marzal, J., 2014. Using Kinect™ sensor in observational methods for assessing postures at work. Appl. Ergon. 45 (4), 976–985.

European Agency for Safety and Health at Work, 2010. OSH in Figures: Work-related Musculoskeletal Disorders in the EU — Facts and Figures. https://osha.europa.eu/en/tools-and-publications/publications/reports/TERO09009ENC (Accessed February 2017).

Hall, M.A., 1999. Correlation-based Feature Selection for Machine Learning. PhD Diss.. The University of Waikato.

Health and Safety Executive, 2016. Work-related Musculoskeletal Disorder (WRMSDs) Statistics, Great Britain. http://www.hse.gov.uk/Statistics/causdis/musculoskeletal/msd.pdf (Accessed February 2017).

Jebelli, H., Ahn, C.R., Stentz, T.L., 2014. The validation of gait-stability metrics to assess construction workers' fall risk. Orlando, FL, June 23-25. In: Proceedings of the 2014 International Conference for Computing in Civil and Building Engineering.

Joshua, L., Varghese, K., 2011. Accelerometer-based activity recognition in construction. Comput. Civ. Eng. 25 (5), 370–379.

Khan, M., Ahamed, S.I., Rahman, M., Smith, R.O., 2011. A feature extraction method for realtime human activity recognition on cell phones. Toronto, Canada. In: Proceedings of the 3rd International Symposium on Quality of Life Technology.

Kilbom, A., 1994. Assessment of physical exposure in relation to Work-Related Musculoskeletal Disorders: what information can be obtained from systematic observations? Scand. J. Work, Environ. Health 30–45.

Liberty Mutual Research Institute For Safety, 2011. Liberty mutual Workplace Safety Index. http://www.coss.net/docs/cosm/ManagingFinances/WorkplaceSafetyIndex2011.pdf (Accessed November 2016).

Lowe, B.D., 2004. Accuracy and validity of observational estimates of wrist and forearm posture. Ergonomics 47 (5), 527–554.

Luinge, H.J., Veltink, P.H., 2005. Measuring orientation of human body segments using miniature gyroscopes and accelerometers. Med. Biol. Eng. Comput. 43 (2), 273–282.

Más, D., Antonio, J., Leal, G., Carolina, D., 2014. Automatizing the management of ergonomic risks prevention using depth sensors. Alcañiz, Spain, July 16–18. In: Proceedings of the 18th International Congress on Project Management and Engineering.

Mathiassen, S.E., Liv, P., Wahlström, J., 2013. Cost-efficient measurement strategies for posture observations based on video recordings. Appl. Ergon. 44 (4), 609–617.

Mourcou, Q., Fleury, A., Franco, C., Klopcic, F., Vuillerme, N., 2015. Performance evaluation of smartphone inertial sensors measurement for range of motion. Sensors 15 (19), 23168–23187.

NIOSH, 2014a. The State of the National Initiative on Prevention through Design. https://www.cdc.gov/niosh/docs/2014-123/pdfs/2014-123.pdf (Accessed February 2016).

NIOSH, 2014b. Observation-based Posture Assessment: Review of Current Practice and Recommendations for Improvement (Publication No. 2014–131).

Occupational Health Clinics for Ontario Workers Inc. Work-related Musculoskeletal Disorders (WMSDs). http://66.51.164.54/resources/handbooks/wrmd/wrmd.pdf (Accessed February 2017).

OSHA, Preventing Sprains, Strains and Repititive Motion Injuries, 2012. https://www.osha.gov/dte/grant_materials/fy11/sh-22310-11/Instructor_Guide.pdf. (Accessed February 2016).

OSHA, Ergonomics for Trainers, 2011. https://www.osha.gov/dte/grant_materials/fy12/sh-23543-12/ErgoforTrainers-TTTProgram.pdf. (Accessed February 2017).

OSHA, Ergonomics:, 2000. The Study of Work. https://www.osha.gov/Publications/osha3125.pdf (Accessed February 2017).

Plantard, P., Auvinet, E., Pierres, A.-S.L., Multon, F., 2015. Pose estimation with a kinect for ergonomic studies: evaluation of the accuracy using a virtual mannequin. Sensors 15 (1), 1785–1803.

Ergonomic-Plus, 2016. http://ergo-plus.com/fundamental-ergonomic-principles/ (Accessed November 2016).

Seel, T., Raisch, J., Schauer, T., 2014. IMU-based joint angle measurement for gait analysis. Sensors 14 (4), 6891–6909.

Shoaib, M., Bosch, S., Incel, O.D., Scholten, H., Havinga, P.J., 2015. A survey of online activity recognition using mobile phones. Sensors 15 (1), 2059–2085.

Simoneau, S., St-Vincent, M., Chicoine, D., 1996. Work-related Musculoskeletal Disorders (WMSDs)- a Better Understanding for More Effective Prevention. IRSST, Québec.

Spielholz, P., Silverstein, B., Morgan, M., Checkoway, H., Kaufman, J., 2001. Comparison of self-report, video observation and direct measurement methods for upper extremity musculoskeletal disorder physical risk factors. Ergonomics 44 (6), 588–613.

Su, X., Tong, H., Ji, P., 2014. Activity recognition with smartphone sensors. Tsinghua Sci. Tech. 19 (3), 235–249.

Teschke, K., Trask, C., Johnson, P., Chow, Y., Village, J., Koehoorn, M., 2009. Measuring posture for epidemiology: comparing inclinometry, observations and self-reports. Ergonomics 52 (9), 1067–1078.

Vignais, N., Miezal, M., Bleser, G., Mura, K., Gorecky, D., Marin, F., 2013. Innovative system for real-time ergonomic feedback in industrial manufacturing. Appl. Ergon. 44 (4), 566–574.

Viikari-Juntura, E., Rauas, S., Martikainen, R., Kuosma, E., Riihimäki, H., Takala, E.-P., Saarenmaa, K., 1996. Validity of self-reported physical work load in epidemiologic studies on musculoskeletal disorders. Scand. J. Work, Environ. Health 22 (4), 251–259.

Winkel, J., Mathiassen, S.E., 1994. Assessment of physical work load in epidemiologic studies: concepts, issues and operational considerations. Ergonomics 37 (6), 979–988.

Wyka, P.M.V., Weira, P.L., Andrewsa, D.M., Fiedlera, K.M., Callaghana, J.P., 2009. Determining the optimal size for posture categories used in video-based posture assessment methods. Ergonomics 52 (8), 921–930.

Yang, L., 2015. Development and Validation of a Novel IOS Application for Measuring Arm Inclination. Thesis. KTH Royal Institute of Technology.

Yang, C.C., Hsu, Y.L., 2010. A review of accelerometry-based wearable motion detectors for physical activity monitoring. Sensors 10 (8), 7772–7788.

Yu, L., Liu, H., 2003. Feature selection for high-dimensional data: a fast correlation-based filter solution. Washington DC. In: Proceedings of the International Conference on Machine Learning.